FEBS Letters 580 (2006) 6730–6740

Trace amounts of copper induce neurotoxicity in the cholesterol-fed mice through apoptosis

Jun Lu[a,b], Yuan-lin Zheng[b,*], Dong-mei Wu[b], Dong-xu Sun[b], Qun Shan[b], Shao-hua Fan[b]

[a] *Institute of Molecular Medicine and Genetics Research Center, School of Basic Medical Science, Southeast University, Nanjing 210009, PR China*
[b] *Key Laboratory for Biotechnology on Medicinal Plants of Jiangsu Province, School of Life Science, Xuzhou Normal University, Xuzhou 221116, PR China*

Received 28 August 2006; revised 26 October 2006; accepted 26 October 2006

Available online 9 November 2006

Edited by Jesus Avila

Abstract **Evidence has been gathered to suggest that trace amounts of copper induce neurotoxicity by interaction with elevated cholesterol in diet. Copper treatment alone showed no significant learning and memory impairments in behavioral tasks. However, copper-induced neurotoxicity was significantly increased in mice given elevated-cholesterol diet. Trace amounts of copper decreased the activity of SOD and increased the level of malondialdehyde (MDA) in the brain of cholesterol-fed mouse. Copper also caused an increase in amyloid precursor protein (APP) mRNA level and the activation of caspase-3 in the brain of cholesterol-fed mice. The apoptosis-induced nuclear DNA fragmentation was detected in the brain of those mice by terminal deoxynucleotidyl transferase (TdT)-mediated dUTP nick-end-labeling staining. These findings suggest that trace amounts of copper induce neurotoxicity in cholesterol-fed mice through apoptosis caused by oxidative stress.**

Keywords: Copper; Cholesterol; Neurotoxicity; Apoptosis

1. Introduction

Copper is an essential metal for all living organisms and is a component of many metalloproteins such as antioxidant enzyme Cu–Zn superoxide dismutase (Cu, Zn, -SOD) and cytochrome oxidase [1,2]. However, copper also plays a role in the pathogenesis of neurodegenerative disease such as Alzheimer's disease (AD) [3]. The amyloid precursor protein (APP) of AD has a copper binding domain (CuBD) located in the N-terminal cysteine-rich region. APP binds to copper with high affinity and reduces Cu(II) to Cu(I) [4–6]. It has been suggested that APP may function as a redox active metalloprotein or as an antioxidant because of its ability to chelate copper ions [7–9].

Cholesterol plays a central role in the development and maintenance of the brain and nervous system [10,11]. Human brain makes up only 2% of the body's weight, yet contains nearly 25% of its cholesterol. But more evidences have implicated a role of cholesterol in AD [11]. According to the cholesterol-Alzheimer's hypothesis, high cholesterol causes the buildup of amyloid plaques, the pathological hallmark of AD [12,13]. The β-amyloid (Aβ) deposition that constitutes the plaques is composed of a 39–42 amino acid peptide, which is the proteolytic product of APP [14,15]. It has been reported that addition of trace amounts of copper to the drinking water of cholesterol-fed rabbits induces accumulation of Aβ and formation of senile plaque (SP)-like structures [16]. Oxidative stress is considered to be involved in the onset and progression of AD. The neurotoxicity of Aβ is also associated with cellular injury following reactive oxygen species (ROS) exposure [17,18]. Application of antioxidants such as Vitamin E has been demonstrated to prevent neurotoxicity from Aβ [19].

Nevertheless, the precise relationship among APP, copper, and cholesterol, and the biochemical role of copper, cholesterol and oxidative stress in neurotoxicity and development of neurodegenerative diseases are still unclear. In this study, the effects of trace amounts of Cu(II) treatment on Cu, Zn-SOD, malondialdehyde (MDA), and the behavior of mice were investigated. The mechanism of neurotoxicity by the cotreatment with Cu(II) and cholesterol was proposed.

2. Materials and methods

2.1. Subjects

Eight-week-old male Kunming strain mice (30.65 ± 4.25 g) were purchased from the Branch of National Breeder Center of Rodents (Shanghai). Prior to experiments mice had free access to food and water and were kept under constant conditions of temperature (23 ± 1 °C) and humidity (60%). Ten mice were housed per cage on a 12-hour light/dark schedule (lights on 08:30–20:30). After acclimatization to the laboratory conditions, mice received a combination of food and water comprising normal chow or normal chow plus 2% cholesterol and distilled water or distilled water plus copper (0.21 ppm) for 8 weeks prior to testing. In brief, mice were divided randomly into 4 groups: (1) control, (2) copper sulfate, (3) cholesterol, and (4) copper sulfate plus cholesterol. All experiments were performed in compliance with the Chinese legislation on the use and care of laboratory animals and were approved by the respective university committees for animal experiments. After the behavioral testing, mice were sacrificed and brain tissues were immediately collected for experiments or stored at −70 °C for later use.

*Corresponding author. Fax: +86 516 83500348.
E-mail addresses: ylzheng@xznu.edu.cn, yzheng170@yahoo.com.cn (Y. Zheng).

Abbreviations: Aβ, amyloid-β peptide; APP, amyloid precursor protein; CuBD, copper binding domain; Cu, Zn,-SOD, Cu–Zn superoxide dismutase; MDA, malondialdehyde; ROS, reactive oxygen species; TUNEL, terminal deoxynucleotidyl transferase (TdT)-mediated dUTP nick-end-labeling

0014-5793/$32.00
doi:10.1016/j.febslet.2006.10.072

2.2. Behavioral tests

2.2.1. Open field test. Based on spontaneous exploration of a novel environment, the open field is one of the most widely used behavioral tests. The open field apparatus was a circular arena (50 cm in diameter, 30 cm in height) made of wood laminated with light-grey resin and illuminated with a single 40 W bulb (3000 lux) placed 2.8 m above the centre of it. The bottom of the arena was divided into 21 equal-area grid cells by white lines. Tests were performed in the breeding room from 8:30 to 16:00 as described previously [20]. The behavioral parameters were analysed as the following: (1) *ambulation*: the number of grids crossed in the arena during the observation period; (2) *rearing*: the number of times the mouse stands on its hind legs; (3) *leaning*: the number of times the mouse placed one or two forelimbs on the wall of the arena; (4) *grooming*: the number of times the mouse 'washes' itself by licking, wiping, combing or scratching of any part of the body.

2.2.2. Step through test. The step-through passive avoidance apparatus consisted of an illuminated chamber (11.5 cm × 9.5 cm × 11 cm) attached to a darkened chamber (23.5 cm × 9.5 cm × 11 cm) containing a metal floor that could deliver footshocks. The two compartments were separated by a guillotine door. The illuminated chamber was lit with a 25 W lamp. The step through test was performed as described previously [20].

2.2.3. Morris water maze. The experimental apparatus consisted of a circular water tank (100 cm in diameter, 35 cm in height), containing water (23 ± 1 °C) to a depth of 15 cm, which was rendered opaque by adding ink. A platform (4.5 cm in diameter, 14.5 cm in height) was submerged 1 cm below the water surface and placed at the midpoint of one quadrant. The pool was located in a test room, which contained various prominent visual cues. The test was performed as described previously [20]. Each mouse received three training periods per day for four consecutive days. Latency to escape from the water maze (finding the submerged escape platform) was calculated for each trial. On day 5, the probe test was carried out by removing platform and allowing each mouse to swim freely for 60 s. The time that mice spent swimming in the target quadrant (where the platform was located during hidden platform training), and in the three non-target quadrants (right, left and opposite quadrants), was measured, respectively. For the probe trials, the number of times crossing over the platform site of each mouse was also measured and calculated. All data were recorded with a computerized video system.

2.3. Preparation of tissue samples

2.3.1. Tissue homogenates. For biochemical studies, animals were deeply anesthetized and sacrificed. Brains were promptly dissected and perfused with 50 mM (pH 7.4) ice-cold phosphate buffered saline solution (PBS). Brains were homogenized in 1/5 (w/v) PBS containing a protease inhibitor cocktail (Sigma–Aldrich, MO, USA) with 10 strokes at 1200 rpm in a Potter homogenizer. Homogenates were divided into two portions and one part was directly centrifuged at 8000 × *g* for 10 min to obtain the supernatant. Supernatant aliquots were used to determine brain MDA levels and protein contents. The second part of homogenates was sonicated four times for 30 s with 20 s intervals using a VWR Bronson Scientific sonicator, centrifuged at 5000 × *g* for 10 min at 4 °C, and the supernatant was collected and stored at −70 °C for determination of superoxide dismutases (SOD) enzyme activities. Protein contents were determined by using the BCA assay kit (Pierce Biotechnology Inc., Rockford, IL).

2.3.2. Collection of brain slice. The mice were perfused transcardially with 25 ml of normal saline (0.9%). The brain tissues were fixed in a fresh solution of 4% paraformaldehyde (pH 7.4) at 4 °C for 4 h, incubated overnight at 4 °C in 100 mM sodium phosphate buffer (pH 7.4) containing 30% sucrose; and embedded in Optimal Cutting Temperature (OCT, Lecia, CA, Germany). Cryosections (12 μm) were collected on 3-aminopropyl-trimethoxysilane-coated slides (Sigma–Aldrich) and stored at −70 °C.

2.4. Assay of SOD activity

Chemicals used in the assay, including xanthine, xanthine oxidase, cytochrome *c*, bovine serum albumine (BSA) and SOD, were purchased from Sigma Chemical Company. SOD activity was measured according to the method described previously [20]. Solution A was prepared by mixing 100 ml of 50 mM PBS (pH 7.4) containing 0.1 mM EDTA and 2 μmol of cytochrome *c* with 10 ml of 0.001 N NaOH solution containing 5 μmol of xanthine. Solution B contained 0.2 U xanthine oxidase/ml and 0.1 mM EDTA. Fifty microliter of a tissue supernatant was mixed with 2.9 ml of solution A and the reaction was started by adding 50 μl of solution B. Change in absorbance at 550 nm was monitored. A blank was run by substituting 50 μl of ultra pure water for the supernatant. SOD levels were expressed as U/mg protein with reference to the activity of a standard curve of bovine Cu, Zn, -SOD under the same conditions.

2.5. Measurement of malondialdehyde (MDA) level

Chemicals: *n*-Butanol, thiobarbutiric acid, 1, 1, 3, 3-tetramethoxypropane and all other reagents were purchased from Sigma Chemical Company. The level of MDA in brain tissue homogenates was determined using the method of Uchiyama and Mihara [21]. Half a milliliter of homogenate was mixed with 3 ml of H_3PO_4 solution (1%, v/v) followed by addition of 1 ml of thiobarbituric acid solution (0.67%, w/v). Then the mixture was heated in a water bath at 95 °C for 45 min. The colored complex was extracted into *n*-butanol, and the absorption at 532 nm was measured using tetramethoxypropane as standard. MDA levels were expressed as nmol per mg of protein.

2.6. RT-PCR and in situ hybridization

2.6.1. RNA isolation, RT-PCR, plasmid construction and in vitro synthesis of riboprobes. The whole brains of mice were dissected after euthanasia with an overdose of the anesthetic agent. Total mRNA was extracted from mice brain with Trizol (Invitrogen, Carlsbad, CA, USA). About 50–100 mg of brain material was used for RNA isolation with 1 ml of Trizol Reagent. AMV reverse transcriptase (Promega, Madison, WI, USA), and oligo-(dT)15 primers (Promega) were used for generating total cDNA. PCR cloning of APP695 (GenBank Accession No. NM_007471) was performed with primers containing *Eco*RI

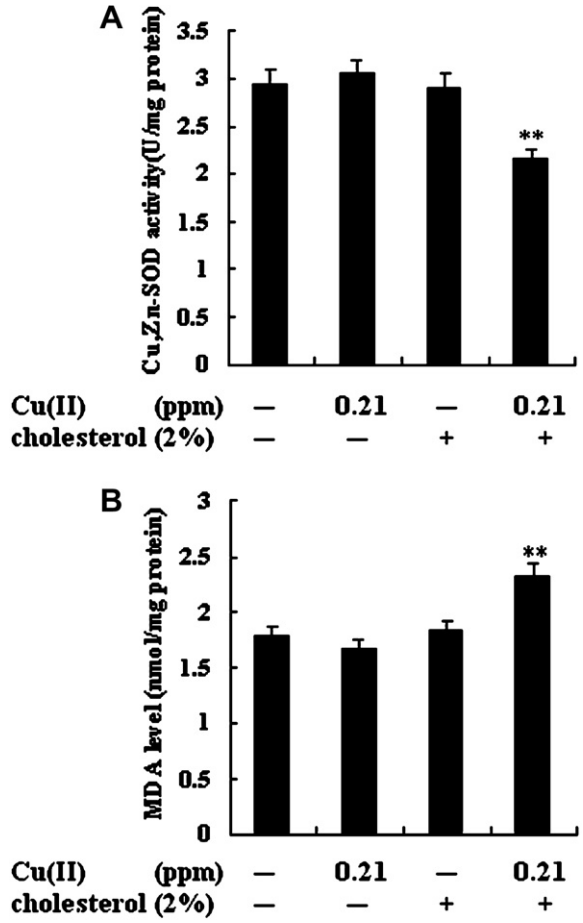

Fig. 1. (A) Trace amounts of copper decrease the SOD activity in the brain of cholesterol-fed mice. (B) Trace amounts of copper increase the MDA level in the brain of cholesterol-fed mice. Data are means ± S.E.M. $^{**}P < 0.01$, as compared to the control group.

(New England Biolab, Beverly, MA) and *Bam*HI (New England Biolab) restriction enzyme cut site. APP mRNA levels were also measured by semi-quantitative RT-PCR [22]. The sequences of PCR primers were as follows:
5′ATC GAATTC CCAACCAGCCAGTGACCATCCAGA 3′ (forward primer)
5′ATC GGATCC CTTCCTCAACATCAGCCACTTCCT 3′ (reverse primer)

For control purposes, levels of β-actin mRNA were measured in the same tubes using the following primers:
5′-TGAACCCTAAGGCCAACCGTGAA-3′ (forward primer)
5′-TCTGCTGGAAGGTGGACAGTGAG-3′ (reverse primer)

The size of the amplified β-actin mRNA fragment was 735 base-pair (bp).

PCR was performed in a reaction volume of 50 μl, using the Expand High-Fidelity PCR-system (Roche Diagnostics Corporation, Indianapolis, IN, USA) according to the instructions of the manufacturer. For PCR, the initial melting temperature was 95 °C for 5 min, followed by 35 cycles at 94 °C for 30 s, 55 °C for 30 s and 72 °C for 1 min, with a final extension at 72 °C for 10 min. The PCR products were visualized on a 1% agarose gel, purified with a Wizard SV Gel and PCR Clean-Up System kit (Promega) and then cloned into pGEM3Z plasmids (Promega). The insert was sequenced and verified to be a 456 bp cDNA, corresponding to bases 408–863 of the APP mRNA. To make APP riboprobe templates, the recombination plasmid containing the 456 bp APP cDNA fragment was linearized with *Eco*RI and transcribed with SP6 RNA polymerase to generate a complementary RNA (cRNA) antisense probe complementary to mouse APP mRNA. A sense probe was generated by linearizing the plasmids with *Bam*HI, and transcribed with T7 RNA polymerase. The antisense and sense (control) riboprobes were labeled by the in vitro transcription in a reaction mixture containing DIG RNA Labeling mix (Roche Diagnostics Corporation), 1 μg of linearized plasmids and 20 units of SP6 or T7 RNA polymerase (Promega) according to the manufacturer's protocol. After transcription, the template DNA was digested with 40 units of DNase I for 15 min at 37 °C. Unincorporated labeling molecules were removed by centrifugation.

2.6.2. In situ hybridization of brain sections. The in situ hybridization was carried out as described (Roche Diagnostics Corporation, Indianapolis, IN, USA), with all steps being performed under RNAse-free conditions prior to hybridization [20]. Hybridization signals were visualized with sheep polyclonal anti-digoxigenin Fab fragments conjugated to alkaline phosphatase using 4-nitro blue tetrazolium chloride and 5-bromo-4-chloro-3-indolyl phosphate as substrates for color reactions in alkaline phosphatase buffer (0.1 M Tris–HCl, pH 9.0, 0.1 M NaCl, 50 mM $MgCl_2$).

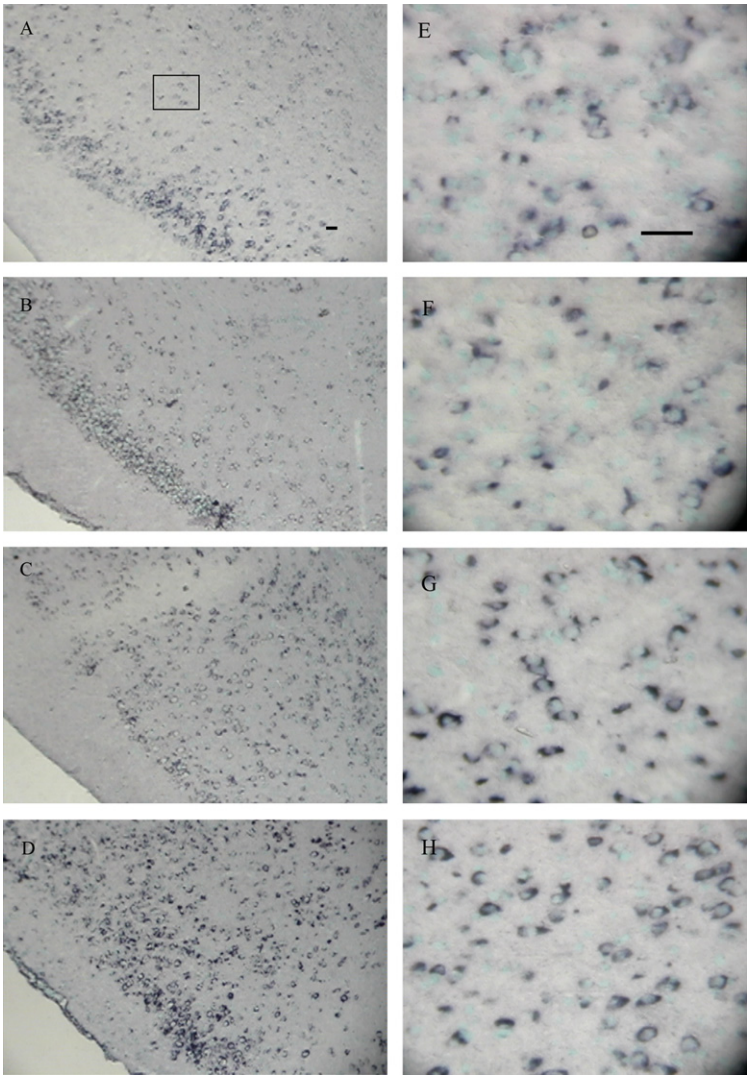

Fig. 2. In situ hybridization analysis of APP mRNA in cerebral cortex of mice. (A) The vehicle control; (B) mice with copper (0.21 ppm) added to their drinking water; (C) cholesterol-fed mice; and (D) cholesterol-fed mice with copper added to their drinking water. The areas indicated in the boxes in panels A, B , C, and D are enlarged in panels E, F, G, and H for clearer visualization. Scale bars: 100 μm (A–H).

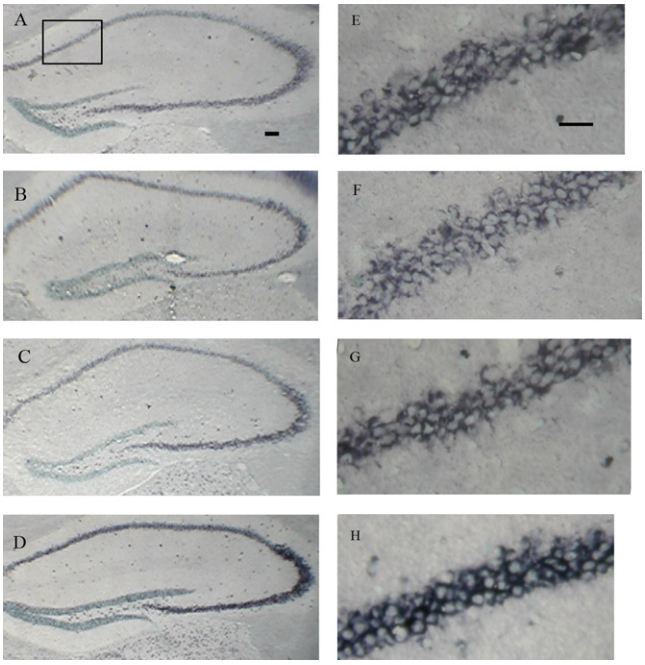

Fig. 3. In situ hybridization analysis of APP mRNA in hippocampus of mice. (A) The vehicle control; (B) mice with copper (0.21 ppm) added to their drinking water; (C) cholesterol-fed mice; and (D) cholesterol-fed mice with copper added to their drinking water. The areas indicated in the boxes in panels A, B, C, and D are enlarged in panels E, F, G, and H for clearer visualization. Scale bars: 100 μm (A–H).

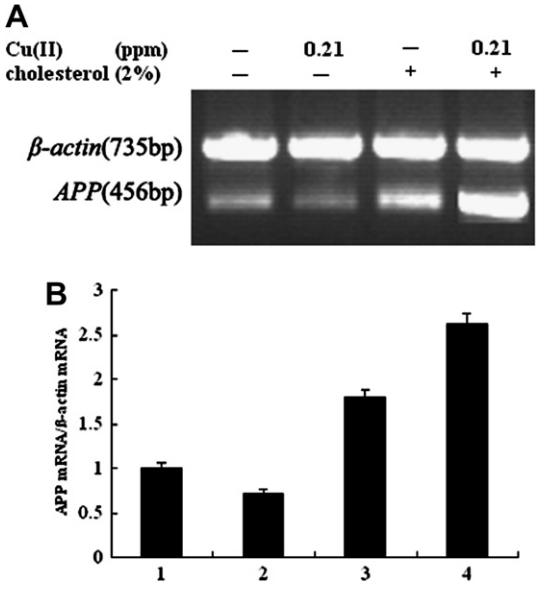

Fig. 4. RT-PCR analysis of the APP mRNA level in mouse brain. (A) The APP mRNA in the brain of the vehicle control, mice with copper (0.21 ppm) added to their drinking water, cholesterol-fed mice, and cholesterol-fed mice with copper added to their drinking water was detected by semi-quantitative RT-PCR; (B) The relative levels of APP mRNA in mouse brain was calculated and expressed as the ratio of APP mRNA to β-actin. Data are means ± S.E.M. (three independent experiments).

2.6.3. RT-PCR analysis. Semi-quantity of detected bands on the agarose gel was calculated using the Scion Image analysis software (Scion Corp., Frederick, MD, USA). Each optical density was normalized using each corresponding β-actin density as an internal control and we standardized the optical density of vehicle control for relative comparison as 1 to compare other groups.

2.7. Immunohistochemistry

Mouse tissues were sectioned after being fixed in 4% paraformaldehyde. For immunohistochemistry, endogenous peroxidase activity in the sectioned tissues was blocked with 3% H_2O_2, and non-specific binding sites were blocked with 3% normal goat serum (Chemicon International Inc., Temecula, CA). The sections were incubated with anti-cleaved caspase-3 (Cell Signaling Technology Inc., Beverly, MA, USA) diluted 1:50 in Tris-buffered saline (TBS) containing 1% goat serum at 4 °C overnight. Subsequently, biotinylated goat anti-rabbit IgG secondary antibody (diluted as per the recommendations of the supplier; Vector Laboratories Inc., Burlingame, CA, USA) was applied, followed by incubation for 1 h with an avidin–biotin–horserad-

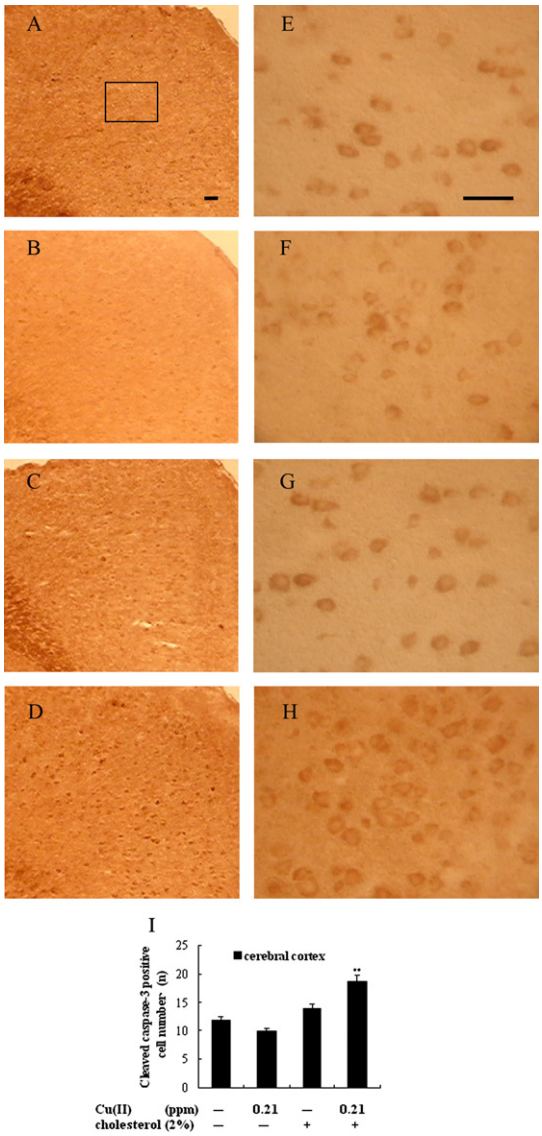

Fig. 5. Immunohistochemistry analysis of activated caspase-3 in the cerebral cortex of mice. (A) The vehicle control; (B) mice with copper (0.21 ppm) added to their drinking water; (C) cholesterol-fed mice; and (D) cholesterol-fed mice with copper added to their drinking water. The areas indicated in the boxes in panels A, B , C, and D are enlarged in panels E, F, G, and H for clearer visualization. Scale bars: 100 μm (A–H). (I) The histogram showed the number of cleaved caspase-3 positive cells in cerebral cortex of mice. Data are means ± S.E.M. ($n = 7$). $^{**}P < 0.01$, as compared to the control group.

ish peroxidase complex (ABC Elite Kit, Vector Laboratories Inc.). Horseradish peroxidase was reacted with diaminobenzidine and H_2O_2 for 5 min to yield a permanent deposit. Stained whole mounts were rinsed in distilled water, mounted on 3-aminopropyl-trimethoxy-silane-coated slides, air-dried overnight, dehydrated in ethanol, cleared in xylene, and cover-slipped with cytoseal (Stephens Scientific, Kalamazoo, MI). The specificity of the staining was assessed by omitting the primary antibody. The number of caspase 3-positive cells in 0.01 mm^2 was estimated by blind manual counting of seven regions located at a consistent position per section.

2.8. TUNEL assay

For terminal deoxynucleotidyl transferase (TdT)-mediated dUTP nick-end-labeling (TUNEL) staining, the standard protocol for frozen sections was followed (BD ApoAlert DNA Fragmentation assay kit, BD Biosciences Clontech, Palo Alto, CA). The sections were immersed in a Coplin jar containing fresh 4% formaldehyde/PBS, and incubated at room temperature for 5 min. The sections were washed twice with PBS for 5 min. The liquid was allowed to drain thoroughly and the slides were placed on a flat surface. Each section was covered with 100 μl of 20 μg/ml Proteinase K solution (Section 3) and incubated at 37 °C for 5 min. After 2 washes of 5 min each with PBS, the sections were transferred into a Coplin jar containing 4% formaldehyde/PBS, and then washed in PBS again. The cells were covered in equilibration buffer (from the kit) and equilibrated at room temperature for 5 min. The equilibrate buffer was drained, and TdT incubation buffer was added to the tissue sections. To perform the tailing reaction, the slice was placed in a dark and humidified 37 °C incubator for 1 h. The tailing reaction was terminated by immersing the samples in 2 × SSC at room temperature for 15 min. Samples were washed three times with PBS for 5 min to remove unincorporated fluorescein-dUTP. Finally, strong, nuclear green fluorescence in apoptotic cells was observed on a fluorescent microscopy (Leica Microscopy Systems, Heidelberg, Germany) equipped with a standard fluorescein filter (520 ± 20 nm). All cells stained with PI exhibit strong red cytoplasmic fluorescence when viewed at 620 nm. The number of TUNEL-positive and total cells in 0.01 mm^2 was estimated by blind manual counting of seven regions located at a consistent position per section. The relative proportion of apoptotic (TUNEL-positive) cells in vehicle control was set as 1.

2.9. Statistic analysis

All statistical analyses were performed using the SPSS software, Version 11.5. Analysis of variance (ANOVA) was carried out with Newman–Keuls or Tukey's HSD post hoc test for multiple comparisons. Data were expressed as means ± S.E.M. Statistical significance was set at $P < 0.05$.

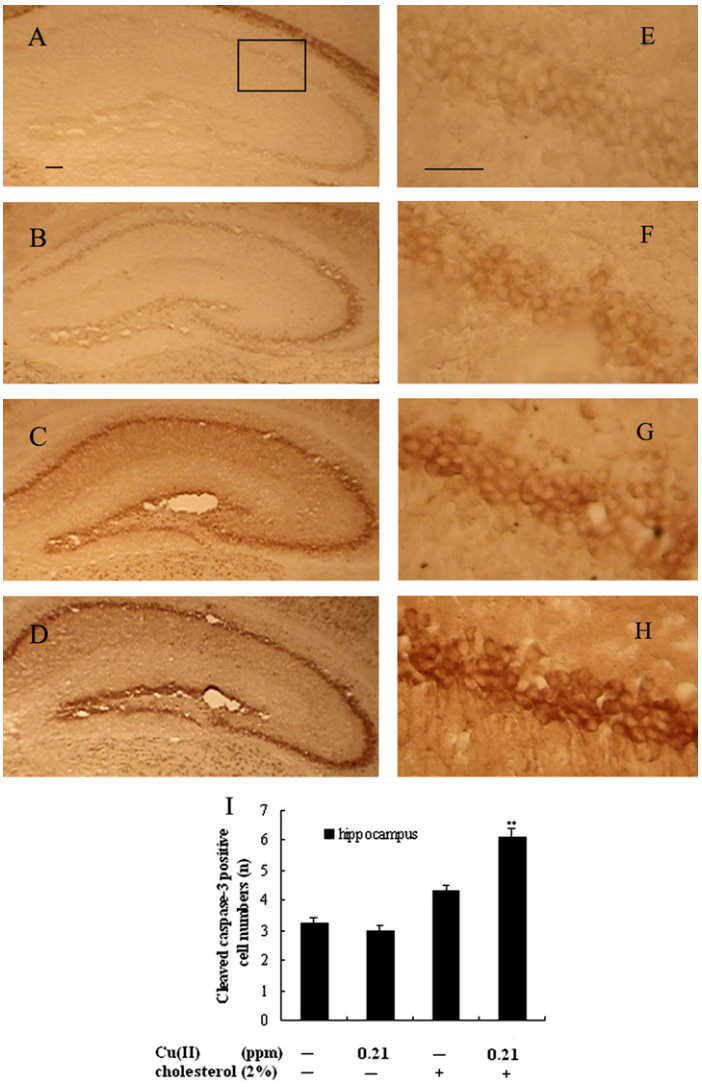

Fig. 6. Immunohistochemistry analysis of activated caspase-3 in the hippocampus of mice. (A) The vehicle control; (B) mice with copper (0.21 ppm) added to their drinking water; (C) cholesterol-fed mice; and (D) cholesterol-fed mice with copper added to their drinking water. The areas indicated in the boxes in panels A, B , C, and D are enlarged in panels E, F, G, and H for clearer visualization. Scale bars: 100 μm (A–H). (I) The histogram showed the number of cleaved caspase-3 positive cells in hippocampus of mice. Data are means ± S.E.M. ($n = 7$). $^{**}P < 0.01$, as compared to the control group.

3. Results

3.1. Copper potentiates the cholesterol-induced decrease in SOD activity and increase in MDA level

Oxidative stress in the brain occurs when the generation of ROS overwhelms the ability of the endogenous antioxidant system including SOD, glutathione peroxidase etc., to remove ROS, subsequently leading to cellular damage. Therefore, low antioxidant capacity could result in brain tissue being susceptible to oxidative damage. Interestingly, copper and cholesterol co-treatment significantly decreased the activity of SOD and increased the level of MDA in the mouse brain, but there were no significant effect by copper or cholesterol treatment alone as compared to distilled water and normal chow treatment (Fig. 1).

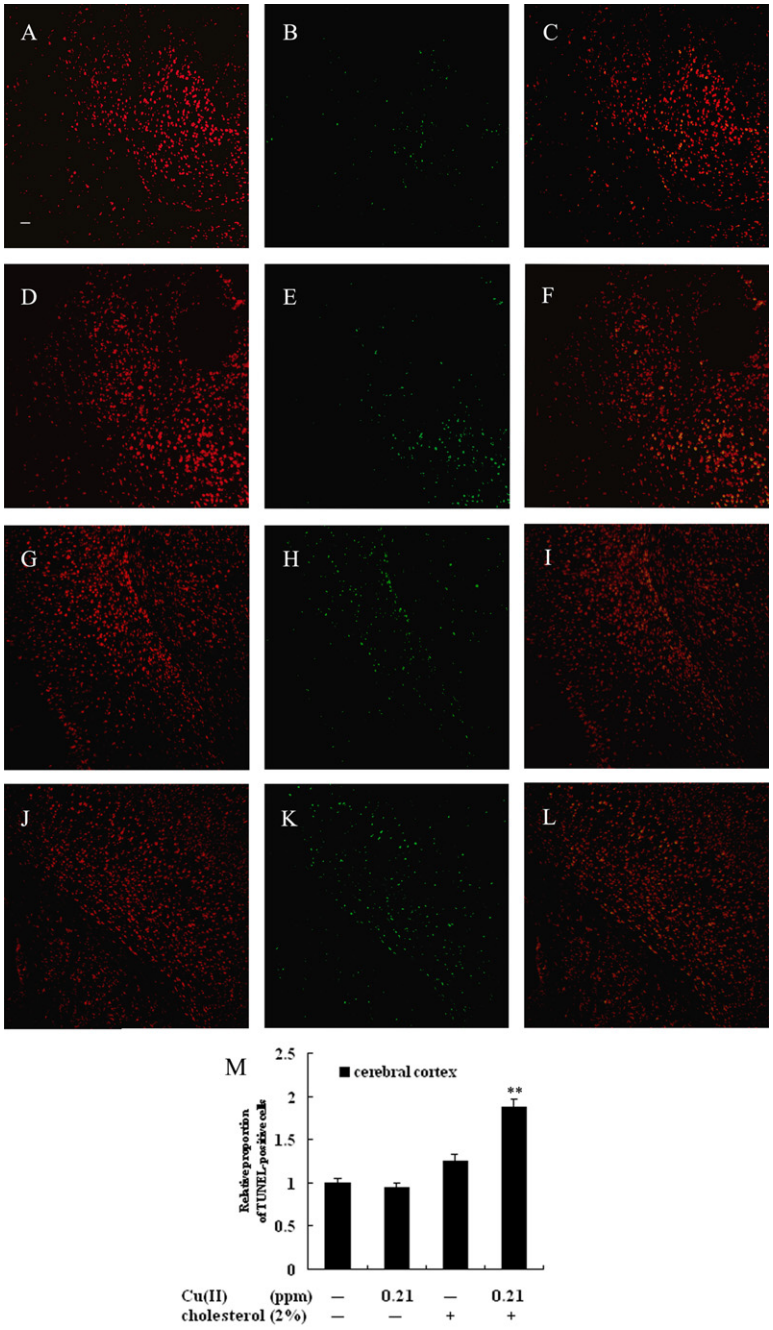

Fig. 7. In situ detection of fragmented DNA (TUNEL assay) in the cerebral cortex of mice. The brain tissues were processed for TUNEL and photographed using a fluorescence microscope with either a propidium iodide (PI) filter alone (left), or a FITC filter alone (middle). (A–C) the vehicle control mice; (D–F) mice with copper (0.21 ppm) added to their drinking water; (G–I) cholesterol-fed mice; (J–L) cholesterol-fed mice with copper added to their drinking water. Apoptotic cells appear fluorescent green with the FITC filter alone (middle). The merged image shows that apoptotic cells appear yellow and non-apoptotic cells appear red (right). Scale bars: 100 μm (A–L). (M) The histogram showed the relative proportion of TUNEL-positive cells in cerebral cortex of mice. Data are means ± S.E.M. ($n = 7$). $^{**}P < 0.01$, as compared to the control group.

3.2. Copper induces the expression of APP mRNA in the brain of cholesterol-fed mice

The expression of APP mRNA in hippocampus and cerebral cortex of mice was analyzed by in situ hybridization and Semi-quantity RT-PCR. The expression of APP mRNA decreased slightly in the cerebral cortex of mice treated with copper alone (Fig. 2). Intriguingly, the same trace amounts of copper significantly induced the expression of APP mRNA in cerebral cortex of cholesterol-fed mice as compared to the control group. The intensified signals were also detected in the CA1, CA2 and CA3 regions of hippocampus (Fig. 3). Consistent with the observations in the cerebral cortex, the copper treatment increased the expression of APP mRNA in the hippocampus of cholesterol-fed mice. Furthermore, Semi-quantitative RT-PCR showed that copper and cholesterol co-treatment increased the level of APP mRNA in the mouse brain (Fig. 4).

3.3. Copper induces the activitation of caspase-3 and apoptosis in the brain of cholesterol-fed mice

Caspase activation has been identified as a hallmark of apoptosis, a form of programmed cell death. Caspase-3, a prototype effector caspase, is able to degrade a number of "death substrates". Activated caspase-3 immunohistochemistry is an

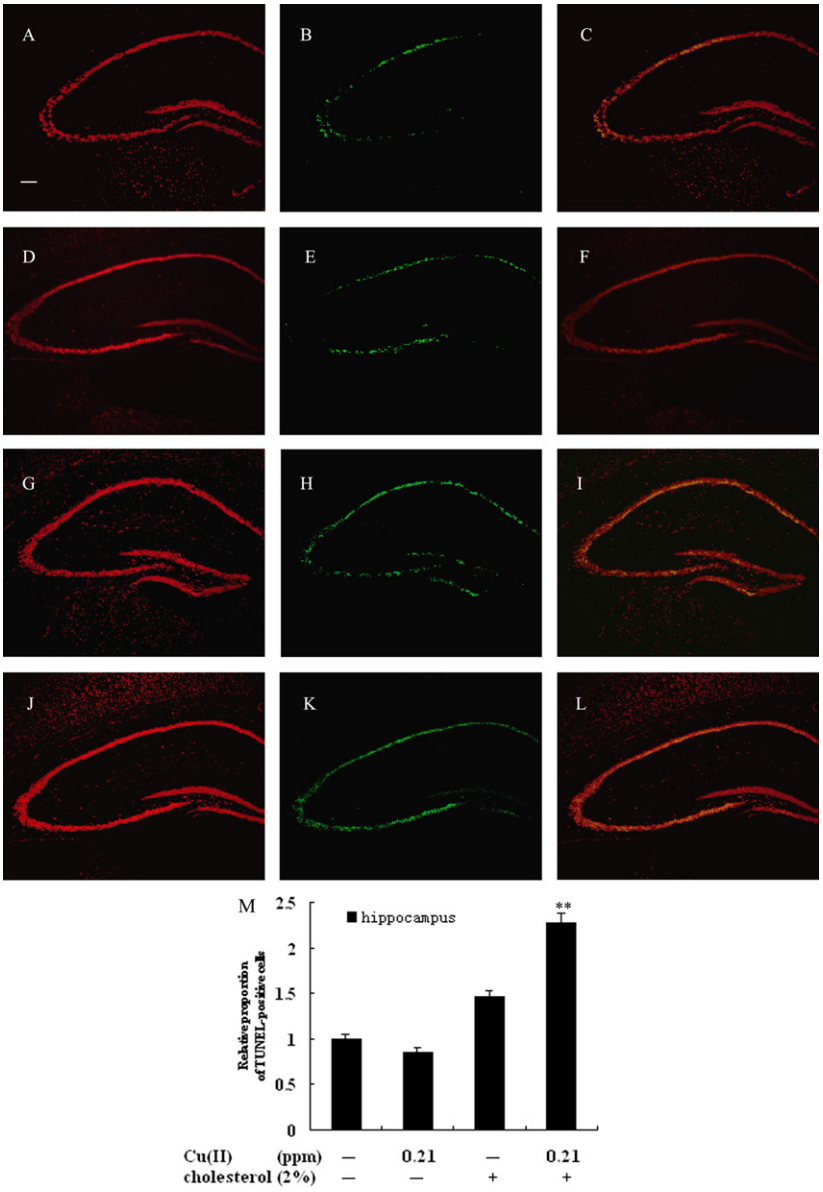

Fig. 8. In situ detection of fragmented DNA (TUNEL assay) in the hippocampus of mice. The brain tissues were processed for TUNEL and photographed using a fluorescence microscope with either a propidium iodide (PI) filter alone (left), or a FITC filter alone (middle). (A–C) the vehicle control mice; (D–F) mice with copper (0.21 ppm) added to their drinking water; (G–I) cholesterol-fed mice; (J–L) cholesterol-fed mice with copper added to their drinking water. Apoptotic cells appear fluorescent green with the FITC filter alone (middle). The merged image shows that apoptotic cells appear yellow and non-apoptotic cells appear red (right). Scale bars: 100 μm (A–L). (M) The histogram showed the relative proportion of TUNEL-positive cells in hippocampus of mice. Data are means ± S.E.M. ($n = 7$). $^{**}P < 0.01$, as compared to the control group.

easy, sensitive, and reliable method for detecting apoptosis. In the cerebral cortex and the hippocampus of mouse brain, we examined the activation of caspase-3 by the method of immunohistochemistry (Figs. 5 and 6). We found that copper treatment alone non-significantly reduced the cleaved caspase-3 positive cells number in the cerebral cortex and the CA1, CA2, CA3 and dentate gyrus regions of hippocampus. Similar to the findings of in situ hybridization of APP mRNA, copper treatment significantly induced the activation of caspase-3 in these brain regions in cholesterol-fed mice [cerebral cortex: $F(3,24) = 9.926$, $P < 0.01$; hippocampus: $F(3,24) = 10.064$, $P < 0.01$].

This study sought further evidence for apoptosis in brain tissue of mice co-treated with copper and cholesterol. Detection of DNA fragments in situ using the TUNEL assay is now commonly used to investigate apoptosis. Enhanced apoptosis was observed in the brain of mice co-treated with trace amounts of copper and elevated cholesterol [cerebral cortex: $F(3,24) = 7.929$, $P < 0.01$; hippocampus: $F(3,24) = 9.591$, $P < 0.01$] (Figs. 7 and 8).

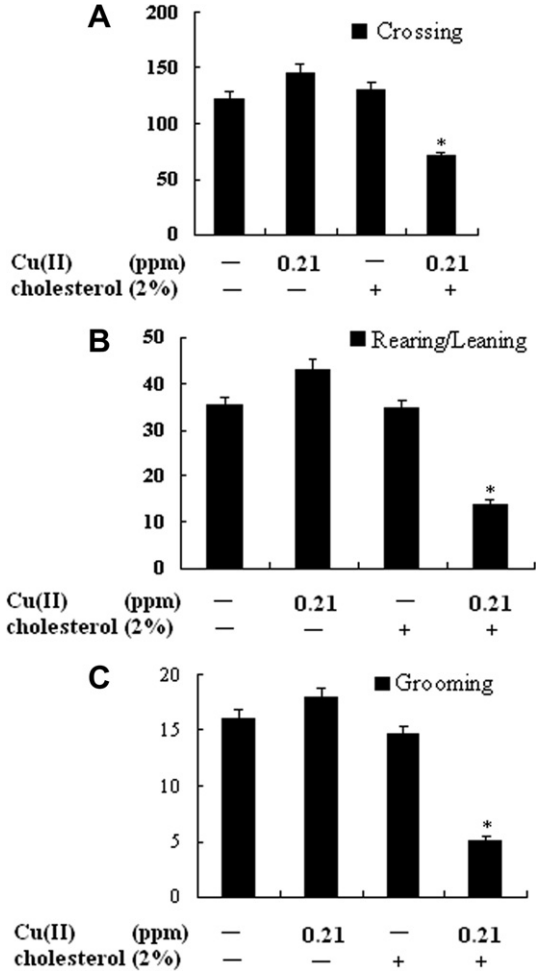

Fig. 9. Open field activity as measured by (A) the number of grid crossing, (B) rearing and leaning, and (C) grooming. All values are expressed as means ± S.E.M. $^{*}P < 0.05$ vs. vehicle control. Scale bars: 100 μm.

3.4. Copper intensifies cholesterol-induced learning and memory impairment

3.4.1. Open field. Open field activity was used to evaluate locomotor activity, exploratory behavior, and anxiety in mice with various treatments. There was a non-significant increase in open field activity in mice with copper added to drinking water, and a decrease in mice with addition cholesterol added to the diet, as compared with mice on distilled water and normal chow. However, significant decrease was found between the mice co-treated with cholesterol and copper and the mice on distilled water and normal chow in grid crossing [$F(3,28) = 6.279$, $P < 0.05$], rearing and leaning [$F(3,28) = 5.575$, $P < 0.05$], and grooming [$F(3,28) = 5.826$, $P < 0.05$], respectively (Fig. 9).

3.4.2. Step through. In the training trial, the latencies for entry into the dark compartment did not differ significantly among groups. In the 72-hour-retention trial, there was no significant difference between the mice treated with either copper or cholesterol and those on normal chow and distilled water. However, the co-treatment of copper and cholesterol significantly decreased the retention latencies [$F(3,28) = 4.239$, $P < 0.05$] (Fig. 10).

3.4.3. Morris water maze. During the training session, all groups of mice improved their performance as indicated by the decreasing escapelatencies across successive days (Fig. 11A). However, the escape latency was generally higher in cholesterol-fed mice given copper in their drinking water than in any other group of mice [day 1: $F(3,28) = 0.635$, $P > 0.05$; day 2: $F(3,28) = 6.183$, $P < 0.05$; day 3: $F(3,28) = 4.190$, $P < 0.05$; day 4: $F(3,28) = 3.867$, $P < 0.05$]. Note that mice of every treatment started at the same level of performance (no significant individual effect was observed for the first three trials of day 1).

The withdrawal of the platform induced a general tendency to swim, preferentially in the quadrant where the platform was previously located as opposed to other quadrants. In terms of relative time spent in the four equivalent quadrants, the ANOVA revealed this preference displayed by all groups except the group co-treated with cholesterol and copper [Control: $F(3,28) = 6.567$, $P < 0.05$; Cu(II): $F(3,28) = 16.161$, $P < 0.001$; Cholesterol: $F(3,28) = 6.816$, $P < 0.05$; Cu(II)/Cholesterol: $F(3,28) = 1.960$, $P > 0.05$] (Fig. 11B). Furthermore, the analysis conducted on the crossings onto the platform zone, in the quadrant where the platform was previously located, revealed

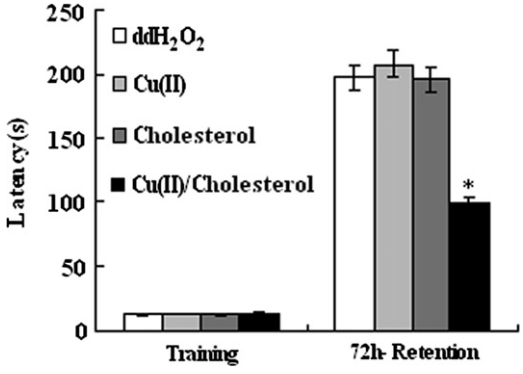

Fig. 10. Performance in the step-through tasks. All values are expressed as means ± S.E.M. $^{*}P < 0.05$ vs. vehicle control. Scale bars: 100 μm.

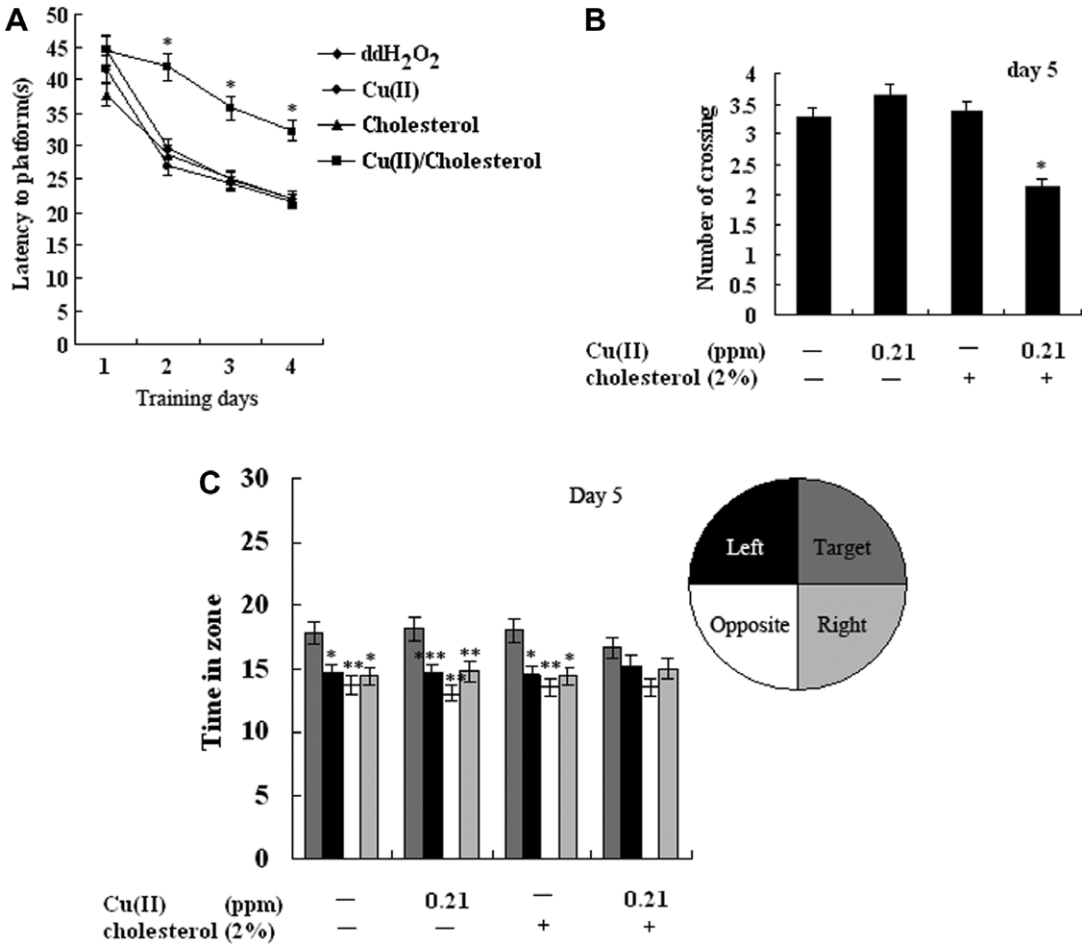

Fig. 11. Performance in the Morris water maze. All values are expressed as means ± S.E.M. (A) Comparison of latencies to platform during 4 training days. (B) Comparison of numbers of crossing over the platform zone on day 5. $^{*}P < 0.05$ vs. vehicle controls. (C) Comparison of the time spent in target quadrant with other quadrants on day5. $^{*}P < 0.05$, $^{**}P < 0.01$, $^{***}P < 0.001$ vs. target quadrant. Scale bars: 100 μm.

a marked preference among controls and mice treated with copper added to the drinking water or cholesterol added to the diet alone (no significant effect); but mice co-treated with copper and cholesterol did not show this preference [$F(3,28) = 5.455$, $P < 0.05$ vs. vehicle control] (Fig. 11C).

4. Discussion

AD is a progressive neurodegenerative disorder characterized by progressive memory impairment as a consequence of loss of synapses and development of amyloid plaques and neurofibrillary tangles. Recent evidence has been gathered to reveal that Aβ precipitation and toxicity in AD are caused by abnormal interaction with metal ions, especially Cu, Zn and Fe. It has been reported that the addition of trace amounts of copper (0.12 ppm) to water given to cholesterol-fed rabbits can induce Aβ accumulation, formation of SP-like structures, and can markedly impair trace conditioning. According to the Environmental Protections Agency maximum contaminant level goal (MCLG) for copper (not exceeds 1.3 ppm) in drinking water, this finding implies that tap water has sufficient copper contamination to impact the pathophysiology of AD. Cholesterol is an integral component of all eukaryotic cell membranes and is essential for normal cellular functions [23,24]. In the nerve system, cholesterol is also vital to the brain and is an important factor in the formation of synapses [25]. However, increasing evidence suggests that excess brain cholesterol plays a role in the pathophysiology of Alzheimer disease (AD) [26]. In our studies, the ANOVA failed to reveal any significant difference in performance among mice treated with copper or cholesterol alone and the controls by behavioral tasks. Interestingly, we found that trace amounts of copper could markedly impair learning and memory abilities of cholesterol-fed mice (Figs. 9–11).

Further studies were carried out to investigate the mechanism of copper-induced neurotoxic effects on the cholesterol-fed mice. The brain is known to possess the highest oxygen metabolic rate of any organ in the body [27]. The transition metals, such as copper and iron, are vital for normal cellular function. However, if not strictly regulated, copper is a potential source of free radical production in the brain [4]. Our result showed that trace amounts of copper could slightly enhance the activity of SOD and reduce the level of MDA in the mouse brain, but these changes were not revealed by ANOVA. Intriguingly, trace amounts of copper facilitated decrease of SOD activity and increase of MDA level in the brain of cholesterol-fed mice. These results indicate that elevated levels of both copper and cholesterol induce brain oxygen damages (Fig. 1).

To prevent transition metal-mediated oxidative stress, cells have evolved complex metal transport systems that deliver Cu and Fe to metalloenzymes and proteins, such as SOD and APP. APP has a copper binding domain (CuBD), which can mediate the oxidative stress in neurons by reducing copper(II) to copper(I) [28]. Furthermore, our results showed that trace amounts of copper could induce higher level of APP mRNA expression than distilled water without copper in the cerebral cortex and the hippocampus of cholesterol-fed mouse (Figs. 2 and 3).

Recent studies also suggest that amyloid-β peptide (Aβ1–42) can sequester copper(II) and prevent the metal ion from generating damaging ROS. It was reported that Cu and Zn are enriched in Aβ deposits in AD patients [29]. Possibly, Aβ is involved in the metal clearance to lower the enhanced level of copper. But the aberrant processing of APP that leads to the aggregation and toxicity of Aβ1–42 is a key molecular event in the pathogenesis of Alzheimer's disease. Consistant with the previous reports, we found that the increase of Aβ was accompanied by the increase of APP mRNA expression (data not shown here).

Caspases are crucial mediators of apoptosis. These enzymes play a dual role in proteolytic processing of APP and the resulting propensity for Aβ deposit, as well as in the ultimate apoptosic death of neurons in Alzheimer disease. APP is directly cleaved within the cytoplasmic tail by caspases, predominantly caspase-3, resulting in the formation of Aβ [30]. Increased level of activated caspase-3 was detected in cerebral cortex and hippocampus of mice co-treated with cholesterol and copper. This may lead to the increased deposition of Aβ and, consequently, the neurotoxicity (Figs. 5 and 6).

Neuronal loss is prominent in certain brain regions in AD patients, and DNA fragmentation in neurons is often used to measure the neuronal loss in a neurodegenerative disease. Using the TUNEL assay, we detected apoptosis-induced fragmented DNA in the brain of cholesterol-fed mice, and the DNA fragmentation was significantly increased by the co-treatment with copper (Figs. 7 and 8). This finding further suggests that the neurotoxicity effect of copper and cholesterol co-treatment is mediated, at least in part, by the apoptosis of neurons.

In conclusion, cholesterol-induced neurotoxicity and deficits in learning and memory abilities could be augmented by cotreatment wih trace amounts of copper, which may be mediated via oxidative stress induced apoptosis.

Acknowledgements: This work is supported by Foundation for University Key Teacher by the Ministry of Education of PR China, Grants from Key Laboratory of Jiangsu Province, Grants from Key discipline of Jiangsu Province and Grants from Qing Lan Project of Jiangsu Province, PR China.

References

[1] Camakaris, J., Voskoboinik, I. and Mercer, J.F. (1999) Molecular mechanisms of copper homeostasis. Biochem. Biophys. Res. Commun. 261, 225–232.
[2] Kroneck, P.H.M., Antholini, W.A., Riester, J. and Zumft, W.G. (1989) The cupric site in nitrous oxide reductase contains a mixed-valence [Cu(II), Cu(I)] binuclear center: a multifrequency electron paramagnetic resonance investigation. FEBS Lett. 242, 70–74.
[3] Multhaup, G., Schlicksupp, A., Hesse, L., Beher, D., Ruppert, T., Masters, C.L. and Beyreuther, K. (1996) The amyloid precursor protein of Alzheimer's disease in the reduction of copper(II) to copper(I). Science 271, 1406–1409.
[4] Barnham, K.J., McKinstry, W.J., Multhaup, G., Galatis, D., Morton, C.J., Curtain, C.C., Williamson, N.A., White, A.R., Hinds, M.G., Norton, R.S., Beyreuther, K., Masters, C.L., Parker, M.W. and Cappai, R. (2003) Structure of the Alzheimer's disease amyloid precursor protein copper binding domain. A regulator of neuronal copper homeostasis. J. Biol. Chem. 278, 17401–17407.
[5] Atwood, C.S., Moir, R.D., Huang, X., Scarpa, R.C., Bacarra, N.M., Romano, D.M., Hartshorn, M.A., Tanzi, R.E. and Bush, A.I. (1998) Dramatic aggregation of Alzheimer Aβ by Cu(II) is induced by conditions representing physiological acidosis. J. Biol. Chem. 273, 12817–12826.
[6] Atwood, C.S., Scarpa, R.C., Huang, X., Moir, R.D., Jones, W.D., Fairlie, D.P., Tanzi, R.E. and Bush, A.I. (2000) Characterization of copper interactions with Alzheimer Aβ peptides: identification of an attomolar affinity copper binding site on Aβ1–42. J. Neurochem. 75, 1219–1233.
[7] Huang, X., Moir, R.D., Tanzi, R.E., Bush, A.I. and Rogers, J.T. (2004) Redox-active metals, oxidative stress, and Alzheimer's disease pathology. Ann. NY Acad. Sci. 1012, 153–163.
[8] Atwood, C.S., Obrenovich, M.E., Liu, T., Chan, H., Perry, G., Smith, M.A. and Martins, R.N. (2003) Amyloid-beta: a chameleon walking in two worlds: a review of the trophic and toxic properties of amyloid-beta. Brain Res. Rev. 43, 1–16.
[9] Kontush, A., Berndt, C., Weber, W., Akopyan, V., Arlt, S., Schippling, S. and Beisiegel, U. (2001) Amyloid-beta is an antioxidant for lipoproteins in cerebrospinal fluid and plasma. Free Radic. Biol. Med. 30, 119–128.
[10] Goritz, C., Mauch, D.H. and Pfrieger, F.W. (2005) Multiple mechanisms mediate cholesterol-induced synaptogenesis in a CNS neuron. Mol. Cell. Neurosci. 29, 190–201.
[11] Dietschy, J.M. and Turley, S.D. (2001) Cholesterol metabolism in the brain. Curr. Opin. Lipidol. 12, 105–112.
[12] Oksman, M., Iivonen, H., Hogyes, E., Amtul, Z., Penke, B., Leenders, I., Broersen, L., Lütjohann, D., Hartmann, T. and Tanila, H. (2006) Impact of different saturated fatty acid, polyunsaturated fatty acid and cholesterol containing diets on beta-amyloid accumulation in APP/PS1 transgenic mice. Neurobiol. Dis. 23, 563–572.
[13] Schneider, A., Schulz-Schaeffer, W., Hartmann, T., Schulz, J.B. and Simons, M. (2006) Cholesterol depletion reduces aggregation of amyloid-beta peptide in hippocampal neurons. Neurobiol. Dis. 23, 573–577.
[14] Rao, K.S.J., Hegde, M.L., Anitha, S., Musicco, M., Zucca, F.A., Turro, N.J. and Zecca, L. (2006) Amyloid beta and neuromelanin – Toxic or protective molecules? The cellular context makes the difference. Prog. Neurobiol. 78, 364–373.
[15] Tanzi, R.E. and Bertram, L. (2005) Twenty years of the Alzheimer's disease amyloid hypothesis: a genetic perspective. Cell 120, 545–555.
[16] Sparks, D.L. and Schreurs, B.G. (2003) Trace amounts of copper in water induced β-amyloid plaques and learning deficits in a rabbit model of Alzheimer's disease. Proc. Natl. Acad. Sci. USA 100, 11065–11069.
[17] Jhoo, J.H., Kim, H.C., Nabeshima, T., Yamadad, K., Shin, E.J., Jhoo, W.K., Kim, W., Kange, K.S., Jo, S.A. and Woo, J.I. (2004) β-Amyloid(1–42)-induced learning and memory deficits in mice: involvement of oxidative burdens in the hippocampus and cerebral cortex. Behav. Brain Res. 155, 185–196.
[18] Pappolla, M.A., Smith, M.A., Bryant-Thomas, T., Bazan, N., Petanceska, S., Perry, G., Thal, L.J., Sano, M. and Refolo, L.M. (2002) Cholesterol, oxidative stress, and Alzheimer's disease: expanding the horizons of pathogenesis. Free Radic. Bio. Med. 33, 173–181.
[19] Subramaniam, R., Koppal, T., Green, M., Yatin, S., Jordan, B., Drake, J. and Butterfield, D.A. (1998) The free radical antioxidant Vitamin E protects cortical synaptosomal membranes from amyloid beta-peptide (25–35) toxicity but not from hydroxynonenal toxicity: relevance to the free radical hypothesis of Alzheimer's disease. Neurochem. Res. 23, 1403–1410.
[20] Lu, J., Zheng, Y.L., Luo, L., Wu, D.M., Sun, D.S. and Feng, Y.J. (2006) Quercetin reverses D-galactose induced neurotoxicity in mouse brain. Behav. Brain Res. 171, 251–260.

[21] Uchiyama, M. and Mihara, M. (1978) Determination of malondialdehyde precursor in tissue by thiobarbituric acid test. Anal. Biochem. 86, 271–278.
[22] Formentin, E., Varotto, S., Costa, A., Downey, P., Bregante, M., Naso, A., Picco, C., Gambale, F. and Lo Schiavo, F. (2004) DKT1, a novel K+ channel from carrot, forms functional heteromeric channels with KDC1. FEBS Lett. 573, 61–67.
[23] Smart, E.J., Ying, Y.S., Conrad, P.A. and Anderson, R.G.W. (1994) Caveolin moves from caveolae to the Golgi apparatus in response to cholesterol oxidation. J. Cell. Biol. 127, 1185–1197.
[24] Murata, M., Peranen, J., Schreiner, R., Weilan, F., Kurzchalia, T. and Simons, K. (1995) VIP21/Caveolin is a cholesterol-binding protein. Proc. Natl. Acad. Sci. USA 92, 10339–10343.
[25] Pfrieger, F.W. (2003) Role of cholesterol in synapse formation and function. BBA-Biomembranes 1610, 271–280.
[26] Wolozin, B., Kellman, W., Ruosseau, P., Celesia, G.G. and Siegel, G. (2000) Decreased prevalence of Alzheimer disease associated with 3-hydroxy-3-methyglutaryl coenzyme a reductase inhibitors. Arch. Neurol. 57, 1439–1443.
[27] Maiese, K. (2002) Organic brain disease in: Encyclopedia of the Human Brain (Ramachandran, V.S., Ed.), first ed, pp. 509–527, Academic Press, San Diego, CA.
[28] White, A.R., Multhaup, G., Maher, F., Bellingham, S., Camakaris, J., Zheng, H., Bush, A.I., Beyreuther, K., Masters, C.L. and Cappai, R. (1999) The Alzheimer's disease amyloid precursor protein modulates copper-induced toxicity and oxidative stress in primary neuronal cultures. J. Neurosci. 19, 9170–9179.
[29] Lovell, M.A., Robertson, J.D., Teesdale, W.J., Campbell, J.L. and Markesbery, W.R. (1998) Copper, iron and zinc in Alzheimer's disease senile plaques. J. Neurol. Sci. 158, 47–52.
[30] Gervais, F.G., Xu, D., Robertson, G.S., Vaillancourt, J.P., Zhu, Y., Huang, J., LeBlanc, A., Smith, D., Rigby, M., Shearman, M.S., Clarke, E.E., Zheng, H., Van Der Ploeg, L.H.T., Ruffolo, S.C., Thornberry, N.A., Xanthoudakis, S., Zamboni, R.J., Roy, S. and Nicholson, D.W. (1999) Involvement of caspases in proteolytic cleavage of Alzheimer's amyloid-beta precursor protein and amyloidogenic A-beta peptide formation. Cell 97, 395–406.